

Tire rolling-resistance computation based on material viscoelasticity representation

Hamad S. Aldhufairi^a and Khamis E. Essa^{*}

Department of Mechanical Engineering, University of Birmingham, Birmingham, B15 2TT, United Kingdom

(Received November 26, 2018, Revised December 11, 2018, Accepted December 12, 2018)

Abstract. Rolling-resistance is growingly driving the focus of many tire research due to its significant impact on the vehicle fuel consumption. The finite element (FE) solution is commonly used as a cost-effective and satisfactory prediction tool compared to the experimental approach. Regardless, the FE choice is still an incomplete work especially in predicting the tire rolling-resistance. This paper investigates the implications of decision between linear (prony) and non-linear (parallel rheological framework (PRF)) viscoelastic models on predicting the tire's rolling-resistance, in particular, and mechanical comfort in FE under different vertical loadings and inflation pressures. The investigation involved following a different way, based on the hysteresis energy ratio, to obtain the rolling-resistance. The PRF model illustrated a good agreement with the experiments and the literature in the estimation of rolling-resistance, dissipative energy distribution and mechanical comfort in tire's structure while prony model had inconsistent and unreasonably small outcomes indicating its insensitivity to rolling.

Keywords: tire; rolling resistance; parallel rheological framework; viscoelasticity; finite element analysis; energy loss

1. Introduction

Fundamentally, the tire rolling-resistance can be viewed as the heat dissipation that occurs in the tire as it deforms during rolling, which can account for up to 20-30% of the total vehicle fuel consumption (Jae 2015). Hereafter, the "rubber" word is used to refer to the vulcanized rubber compounds of the tire. The viscoelasticity of tire rubber (i.e., material hysteresis) is proven to be a key factor whenever the tire rolling-resistance is to be estimated. This is because the viscoelasticity can contribute up to 80-95% of the tire rolling-resistance compared to secondary factors like aerodynamic drag and road friction (i.e., ~15% and ~5% of rolling-resistance respectively) for a steady-state rolling case on flat ground (Redrouthu and Das 2014).

Attempts were made to describe such viscoelastic behavior, which of non-linear nature, in many studies to predict the tire rolling-resistance using finite element analysis (FEA) as a cost-

^{*}Corresponding author, Ph.D., E-mail: K.E.A.Essa@bham.ac.uk

^aPh.D. Student, E-mail: hsa345@bham.ac.uk

effective, time-saving and satisfactory alternative to the costly experimental method (Andersen *et al.* 2014). Different researchers have followed diverse ways to determine the tire rolling-resistance as either “drag force” or “energy lost per a unit distance” (Hoever 2014, Andersen 2015). The latter definition is widely used as it is more comprehensive and applicable (Ghosh 2011, Schuring 1977). Commonly, one of two approaches is used to compute the tire energy dissipation either through a “viscoelastic theorem in a post-FEA processing code” or “viscoelastic material model of the FEA solution”.

For the “viscoelastic theorem”, the approach would usually involve the usage of a commercial FE code with an in-house developed code (Ghosh *et al.* 2003). The in-house developed codes are usually adopted as a post-FEA processing tool to use the time histories of the stress-strain cycles in the FE tire model with experimental material loss properties to determine the rolling-resistance through applying the proposed viscoelastic theorem. Many research works followed that approach like that of Ghosh (2011), Cho *et al.* (2013) and Hoever (2014).

Most of the existent “viscoelastic theory” investigations usually utilize in-house developed codes that are not available for commercial usage. Another limitation is the implementation of “linear viscoelasticity” hypotheses to simplify the description of the tire rubbers that are of highly non-linear nature (Nandi *et al.* 2014). Furthermore, the viscoelastic theorem normally consists of a lengthy dynamic analysis of the tire involving several assumptions taken to reach an approximate solution with limited accuracy. This theorem is usually coupled with static-contact FE models, and it is more difficult to be coupled with the dynamic rolling conditions.

For the “viscoelastic models within the FEA solution”, the majority of the available works such as that of Ghosh *et al.* (2003) and Hernandez *et al.* (2017) use a linear viscoelastic measure for the highly non-linear viscoelasticity of the tire rubbers. In these models, the viscoelastic property depends on the deformation orientation, strain amplitude, and response cycles from which limits from its applicability. Accordingly, the default viscoelastic model solely may not be enough to estimate the rolling-resistance unless it is fitted against several experimental strain or loading frequency cycles, built on the relevant deformational mode, or aided with the necessary analytical formulas. Another issue is the compromise between solution accuracy, problem complexity, and computational costs.

For the tire manufacturers, a more experimentally based approach is used to estimate the tire’s rolling-resistance than the FE approach given the output accuracy, the testing comprehensiveness, and the needed resources availability despite the costs incurred (Ghosh 2011). However, growingly utilized, their FE modeling is usually in-house built and confidential as it would contain sensitive information of their tires and their competitive-edge techniques (Heeps 2015, Steen 2010, Smith and Blundell 2017).

The above literature reveals that the tire FE modeling for the rolling-resistance is still an incomplete job and further development is yet needed. This is due to the limited accuracy as a result of the complex relationship between the hysteresis loss and the rolling-resistance which is further complicated by the operational conditions and the tire design aspects (Aldhufairi and Olatunbosun 2017).

Consequently, this paper explores the impact and the possibility of using a non-linear viscoelastic model (i.e., PRF) within the FEA solution, instead of the traditional linear viscoelastic model (i.e., prony) or the linear-based viscoelastic theorems, in describing the tire’s core rolling-resistance (due to material hysteresis) and mechanical comfort. To achieve that, Abaqus/Explicit was used to run a 3D tire FE model and obtain the relevant energy outputs and vibrational forces to compute the tire’s rolling-resistance and the mechanical comfort respectively. Under steady-

state free-rolling conditions, the FE outcomes for both PRF and prony models were validated against the corresponding experiments with a focus on rolling-resistance as the main performance measure.

In this context, the paper will be presenting a brief background on tire's rolling-resistance, the material property acquisition, the experimental set-up, the tire FE model development, the rolling-resistance computation with different material models, and the applicability of the FE model to predict tire's rolling-resistance and mechanical comfort.

2. Material properties acquisition

In this study, a 225/55 R17 radial passenger-car tire was used for the investigation. To model the non-destructive mechanical response of the tire using FE, the hyperelastic and viscoelastic properties of the rubbers are needed with the elastic properties of the reinforcements (Yang 2011, Wei 2015).

2.1 Hyperelasticity

The hyperelasticity is the elastic response (i.e., energy restored) of the viscoelastic rubber (Systèmes 2013a). This behavior is accompanied with the consideration of rubber as isotropic and nearly incompressible material. To capture the elastic response, the nominal stress-strain experimental data were obtained for the different tire rubber components (i.e., tread, sidewall, and apex/chafer) through conducting a simple uniaxial tensile test. The method used to extract the rubber samples, pre-condition and test them is similar to that done by ASTM D412-15a standard (ASTM 2016).

In this paper, Abaqus 6.13-1 is used as the commercial FE platform for the tire modeling. Abaqus was used to fit the possible hyperelastic models for rubber elasticity representation against the obtained experimental data through the "least-squares fitting" technique. Yeoh model was found to have the best data-fit along being applicable to the other deformational modes and has low experimental acquisition cost. Therefore, Yeoh model was chosen to represent the rubber hyperelasticity (Systèmes 2013a)

$$U = C_{10}(\bar{I}_1 - 3) + C_{20}(\bar{I}_1 - 3)^2 + C_{30}(\bar{I}_1 - 3)^3 + \frac{1}{D_1}(J^{el} - 1)^2 + \frac{1}{D_2}(J^{el} - 1)^4 + \frac{1}{D_3}(J^{el} - 1)^6 \quad (1)$$

Where:

U = Strain Energy Stored per Unit Volume.

C_{i0} and D_i = Material Coefficients.

\bar{I}_1 = First Deviatoric Strain Invariant.

J^{el} = Elastic Volume Ratio.

From Abaqus, the following long-term Yeoh hyperelastic material coefficients were obtained:

Table 1 Yeoh coefficients for tire rubbers

Rubber Part	Yeoh Model Parameters		
	C10	C20	C30
Tread	0.96	-0.28	9.01E-02
Sidewall	0.48	-0.11	2.86E-02
Apex	1.57	-1.38	0.92

2.2 Linear viscoelasticity

For linear viscoelasticity, Abaqus uses Prony series to model the time-domain viscoelastic material property. To calculate Prony series coefficients, a “stress-relaxation test” was conducted at 50% strain level for the same rubber samples. The method used to precondition and test these rubber samples conforms to ASTM E328-13 Standard (ASTM 2014). Abaqus was used to calculate and fit the following “Prony series expansion” against the experimental data using a non-linear least-squares-fit technique (Systèmes 2013b)

$$g(t) = 1 - \sum_{i=1}^N \bar{g}_i (1 - e^{-t/\tau_i}) \quad (2)$$

Where:

$g(t)$ = Normalised Relaxation Modulus.

\bar{g}_i = Prony Series Coefficient.

t = Experiment Time.

τ_i = Relaxation Time.

N = Term Number.

The computed Prony series coefficients (\bar{g}_i, τ_i) are given in Table 2 for all the rubber samples.

Table 2 Prony coefficients for tire rubbers

Rubber Part	Prony Model Parameters					
	\bar{g}_1	τ_1	\bar{g}_2	τ_2	\bar{g}_3	τ_3
Tread	3.28E-02	12.58	3.58E-02	88.42	3.69E-02	651.45
Sidewall	4.44E-02	56.69	3.52E-02	932.71		
Apex	2.97E-02	11.48	3.80E-02	88.34	3.93E-02	781.59

2.3 Non-linear viscoelasticity

To predict the tire’s non-linear viscoelasticity, the PRF model is used. For a reversible deformation, the PRF model comprises of a pure elastic network and multiple viscoelastic networks connected all together in parallel. The pure elastic network is represented by the Yeoh hyperelastic model to describe the large non-linear elastic deformations and prevent complete stress relaxation. For the viscoelastic networks, each network is defined by a multiplicative

division of the “deformation gradient” into an “elastic part” and a “viscous part”. The “elastic part” for each network is specified by the same Yeoh model after being scaled by every network’s stiffness ratio. For the “viscous part”, it can be described through the usage of the following “flow rule” and “evolution law” (Systèmes 2013c)

Flow Rule

$$D^{cr} = \frac{3}{2\bar{q}} \dot{\bar{\epsilon}}^{cr} \bar{\sigma} = \frac{3}{2\tilde{q}} \dot{\bar{\epsilon}}^{cr} \bar{\tau} \tag{3}$$

Evolution Law: Power-law Strain Hardening Model

$$\dot{\bar{\epsilon}}^{cr} = \left(A\tilde{q}^n [(m + 1)\bar{\epsilon}^{cr}]^m \right)^{\frac{1}{m+1}} \tag{4}$$

Where:

D^{cr} = Symmetric Part of Velocity Gradient.

\bar{q} = Equivalent Deviatoric Cauchy Stress.

$\bar{\sigma}$ = Deviatoric Cauchy Stress.

\tilde{q} = Equivalent Deviatoric Kirchhoff Stress.

$\bar{\tau}$ = Deviatoric Kirchhoff Stress.

A , m and n = Material Constants.

$\bar{\epsilon}^{cr}$ = Equivalent Creep Strain.

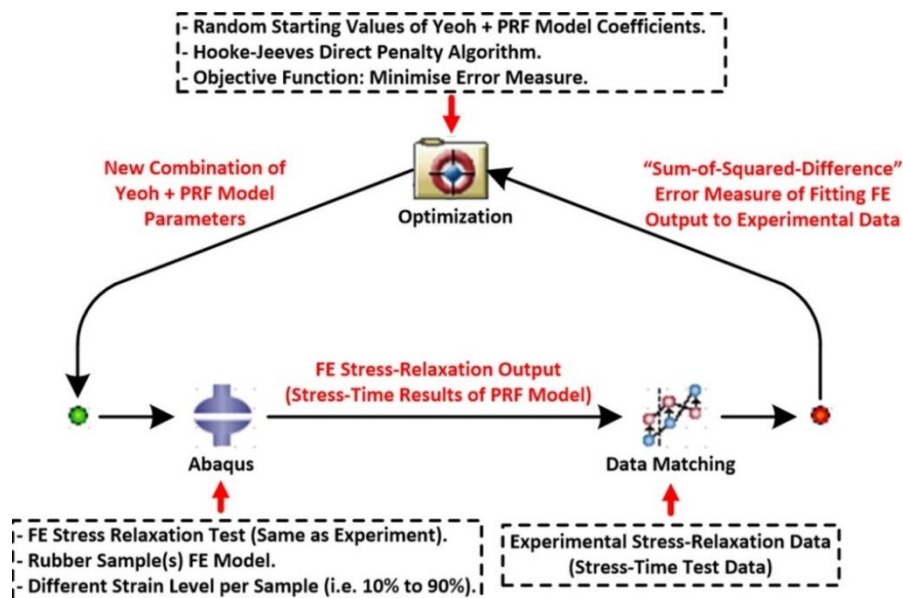


Fig. 1 Isight optimisation model

To use the PRF model in Abaqus, the Isight 5.9.4 calibration model in Fig. 1 was built and used to calculate and fit the PRF coefficients against the experimental stress-relaxation test data for the

same rubber samples but at different strain levels to capture the material’s non-linearity. The following Table 3 and Fig. 2 illustrate the optimized Yeoh and PRF parameters and an example of the optimization results for the tread sample respectively:

Table 3 Optimized Yeoh and PRF model parameters for all rubbers

Material Model Parameters		Tire Rubber Component(s)		
		Tread	Sidewall	Apex
Yeoh	C10	0.64	0.39	0.79
	C20	-0.07	-0.03	-0.15
	C30	0.03	0.009	0.15
PRF	SR1	0.40	0.12	0.0001
	SR2	0.03	0	0.39
	SR3	0.007		0.04
	A1	3.87	0.76	0.16
	n1	4.04	2.72	1.05
	m1	-0.65	-0.13	-0.01
	A2	0.30	0.04	1.50
	n2	2.77	1.22	6.50
	m2	-0.007	-0.33	-0.35
	A3	0.36		0.05
	n3	1.21		3.14
	m3	-0.0004		-0.0004

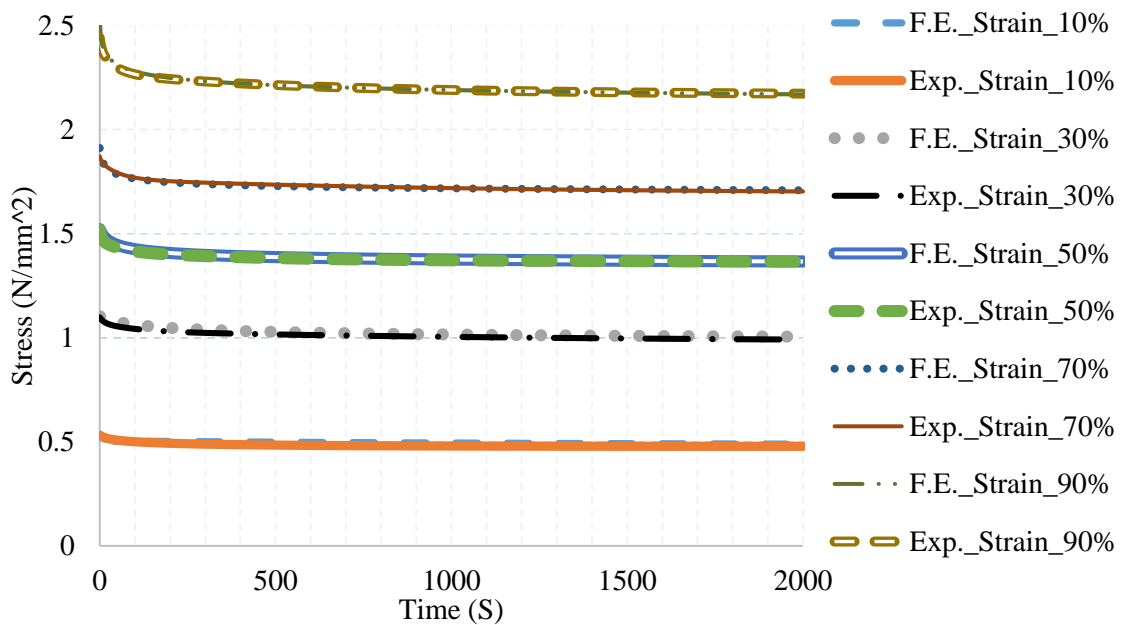


Fig. 2 Tread stress-relaxation for optimized PRF model and experimental test

3. Experimental testing of tire

A series of experimental tests were carried out using a “tri-axial electro-hydraulic tire/drum test rig”, as seen in Fig. 3, to measure the tire’s rolling-resistance and mechanical comfort.



Fig. 3 Tri-axial tire/drum test rig

The experimental measurements of the rolling-resistance, under the steady-state and straight free-rolling conditions specified in Table 4, were carried-out according to ISO 18164:2005 standard in terms of the testing/measurement procedures and the data analysis/interpretation except for the earlier rolling conditions to meet the paper’s goal(s) (ISO 2005).

Table 4 Investigated tire rolling conditions

Relationship Investigated		Fixed Parameters		Variable Parameters
Testing Scope	Rolling-Resistance VS Load	Rolling Velocity (Kph)	Inflation Pressure (KPa)	Vertical Load (KN)
		30	220	1, 2, 3, 4 and 5
	Rolling-Resistance VS Pressure	Vertical Load (KN)	Rolling Velocity (Kph)	Inflation Pressure (KPa)
		4	30	180, 200, 220, 240 and 260

As indicated, the rolling-resistance tests were carried-out at a fixed low rolling velocity to exclude the effect of the “aerodynamic drag” on the tire’s rolling-resistance (Clermont-Ferrand 2003, Katz 2016). This is as this paper’s focus is on measuring the rolling-resistance related to the tire’s internal losses due to the material’s hysteresis during normal tire deformation at the contact-patch. For this purpose, free-rolling conditions on a smooth road-drum were adopted for the tests to eliminate or substantially minimize the effects of traction, braking and road-surface roughness on the tire’s rolling-resistance. Also, a skim test was done according to ISO 18164:2005 to measure and exclude any parasitic energy losses other than the tire’s internal losses.

The “test rig” was used to measure the longitudinal force at the tire spindle where this force

was transformed later to the rolling-resistance through Eq. (5) below.

$$E_{RR} = F_t \cdot \left(1 + \frac{r_L}{R}\right) \quad (5)$$

Where:

E_{RR} = Energy Loss per Unit Distance.

F_t = Longitudinal Force at Tire Centre.

r_L = Loaded Tire Radius.

R = Drum Radius.

Under similar rolling conditions, the “variations in both vertical and lateral forces” were calculated after reconfiguring the test rig to measure both vertical and lateral forces at the tire spindle according to Michelin (Michelin 2002).

4. Development of FE tire model

To model the tire structure in FE, a cross-sectional sample of the tire was extracted from the actual tire, and its 2D profile was captured. Based on the 2D profile, a 2D axisymmetric model of the tire’s rubber and reinforcement components was made in Abaqus/CAE as shown in Fig. 4. For a more manageable FE model, a “pattern-less” tire profile was adopted to reduce hour-glassing effect considerably as this has insignificant influence over rolling-resistance.

The reinforcements were modeled as rebar-layers with surface elements (SFMGAX1). The rubbers were modeled as shells with solid elements (CGAX4R). The reinforcements were embedded within the relevant hosting rubber parts. The wheel rim was modeled by creating a reference-point representing the wheel hub center and tying-up this point with the relevant tire/rim contact nodes as a rigid-body.

Implementing the “symmetric model generation” and “symmetric results transfer” techniques in Abaqus/Standard, the 2D axisymmetric tire model was revolved into a full 3D model. An Abaqus “input” file was produced containing the model data with an analytical rigid surface drum acting as the road as seen in Fig. 4.

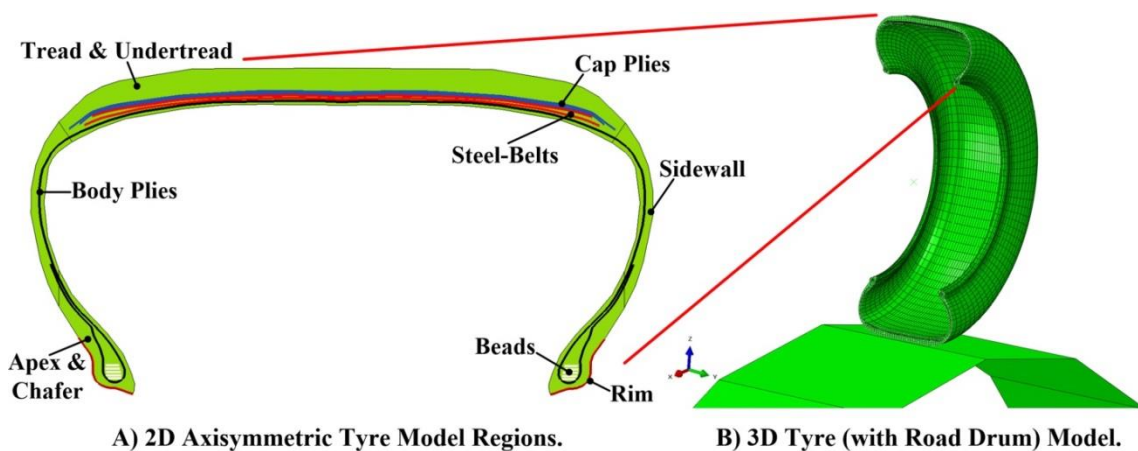


Fig. 4 2D and 3D tire FE models

A mesh convergence analysis was performed for the 3D tire model to find out the proper circumferential mesh density with the minimal computational cost possible that would give consistent and accurate FE solution. The full 3D FE model of the tire comprised of 66103 nodes and 57305 elements.

5. FE simulation

The Abaqus “input” file, created earlier, was updated with the necessary analysis steps to run the targeted tire rolling settings corresponding to the experimental testing. Two sets of rolling-resistance simulations were created. The first is to investigate the rolling-resistance using the linear viscoelasticity (i.e., Prony model), and the other one is using the non-linear viscoelasticity (i.e., PRF model).

For the Prony model, the rolling-resistance simulation was performed using multiple steps and analysis procedures. Using Abaqus/Standard, two static load steps were created where viscoelastic effects are negligible. The first step involved inflating the tire. In the second step, the tire was brought into initial contact with the drum, and a vertical load was applied to the tire against the drum. A steady-state transport step was created, as a third step, to apply an angular velocity condition to the drum to rotate the tire in a free-rolling steady-state due to its contact with the drum. Using the “import” feature, the simulation results were transferred from Abaqus/Standard to Abaqus/Explicit. A dynamic step was introduced to continue rolling the tire at a free-rolling steady-state through moving the drum by the prescribed angular velocity.

For the PRF model, the rolling-resistance simulation was carried-out using several dynamic steps in the Abaqus/Explicit only since the PRF model is not compatible for usage with the “steady-state transport” and the “import” techniques. The tire inflation and then vertically loading it were done quasi-statically in the first and second steps respectively to eliminate dynamic effects. The last step involved steady-state free-rolling the tire through rotating the drum at the specified angular velocity.

To minimize the noises for better results in the explicit dynamic analysis, a “contact damping” function was implemented, as a fraction of the model critical damping, in the general contact interaction of the tire/drum in the velocity step.

6. Rolling-resistance computation

In this paper, the rolling-resistance is described as “energy lost per a unit distance” since it gives a more comprehensive definition and applicable especially as a free-rolling case is being investigated. For computational efficiency, in Fig. 5, this paper proposes determining the tire’s rolling-resistance based on the tire’s hysteresis ratio and the work done by the tire at the contact-patch region calculated through the relevant FE outputs.

From FE modeling, once the tire reaches a steady-state rolling condition, the tire’s hysteresis ratio could be found through the gradient of the tire’s dissipation energy against that of its internal energy (i.e., ALLCD/ALLIE). At the contact-patch, the tire’s (stored) energy could be quantified through calculating the work performed by the tire on the contact-patch via the product of the tire’s contact force and its vertical deflection. The energy consumed (lost) by the tire for traveling a distance equivalent to the contact-patch’s length was obtained from the multiplication of the

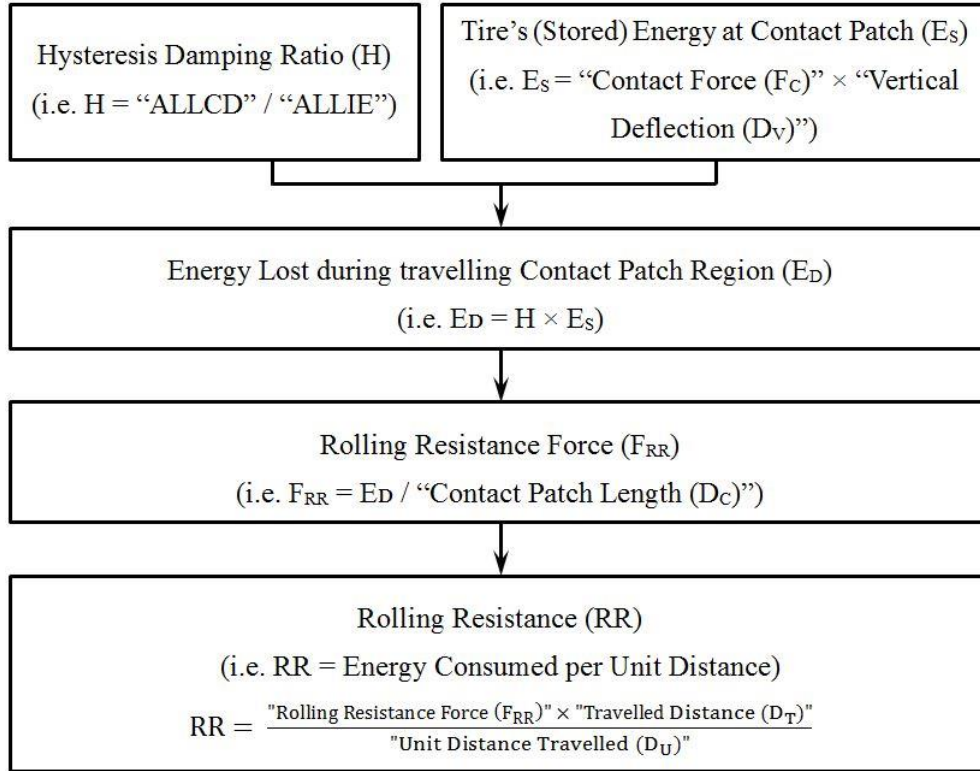


Fig. 5 Rolling-resistance computation approach

hysteresis ratio with the tire's (stored) energy at the contact-patch. Based on that, the tire's rolling-resistance force could be specified through the division of the energy lost at the contact-patch over the patch's length. Under the same rolling conditions, for any given traveled distance, without the need to literally modeling it in FE, the tire's rolling-resistance, as energy per unit distance, can be determined based on the rolling-resistance force as follows

$$RR = \frac{\text{Rolling Resistance Force} \times \text{Travelled Distance}}{\text{Unit Distance Travelled}} \quad (6)$$

7. Results and discussion

7.1 Rolling-resistance

Prior to analyzing the end results, an initial check-up for FE model's response validity and accuracy was made through evaluating the "total energy of the whole FE model (ETOTAL)" and the "ratio of the artificial strain energy (ALLAE) to the total strain energy (ALLIE)" for the FE tire model as well (Systèmes 2013d). The total energy (ETOTAL) was found almost constant, for both PRF and prony models, indicating the complying of the FE modeling with the law of

conservation of energy. Again, for both PRF and prony models, the “artificial energy” (ALLAE) was found to be nearly around 4-5% of the “tire’s internal energy” (ALLIE) implying negligible hourglassing effects, stable FE model and that the physical process of the tire’s rolling is being simulated properly.

For the rolling-resistance results, the following FE and experimental results in Figs. 6 and 7 were reached after applying the methodologies specified in sections (6) and (3). From a glance, the PRF model is considered a better choice than the Prony model in describing the tire’s rolling-resistance. The prony model gave unreasonably very small rolling-resistance levels compared to practice. In that regard, tire rolling simulation is a highly non-linear FE problem whether it was for tire’s geometry, contact/boundary conditions or material behavior (Li *et al.* 2012). Given both PRF and prony models share the same FE tire model in terms of geometry, construction and contact/boundary conditions, apparently, the reason behind such rolling-resistance results was the material module adopted.

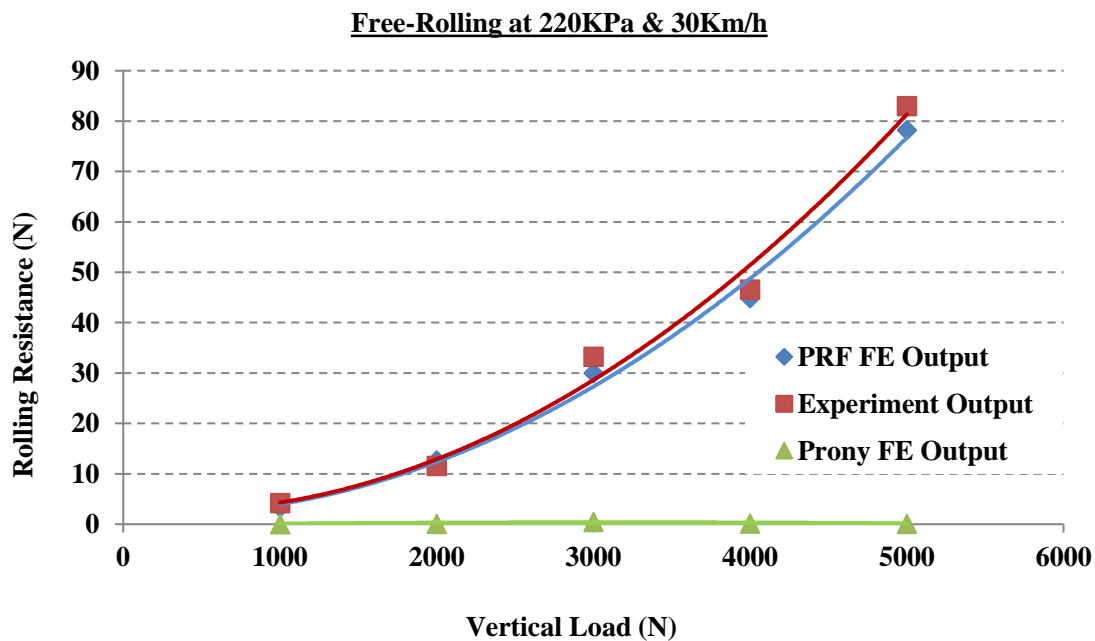


Fig. 6 Effects of vertical load over rolling-resistance

Prony series, as a linear viscoelastic model, was found to produce unreliable and inconsistent creep dissipation energies of the tire irrespective of the given rolling conditions. An example on that can be seen in the dissipation energy distribution between the tire’s main components in Fig. 8 later in this section. This means the prony model is not compatible in accounting for the tire’s non-linearity and different deformational levels when computing tire’s dissipative energy.

A closer look at the prony viscoelastic model reveals the independence of its shear elastic modulus to the applied stress and induced strain with a linear representation of the relationship between the stress and strain responses. Such a situation is only valid and possible with ideal materials and where the deformation in the system is either very small or happens very slowly in

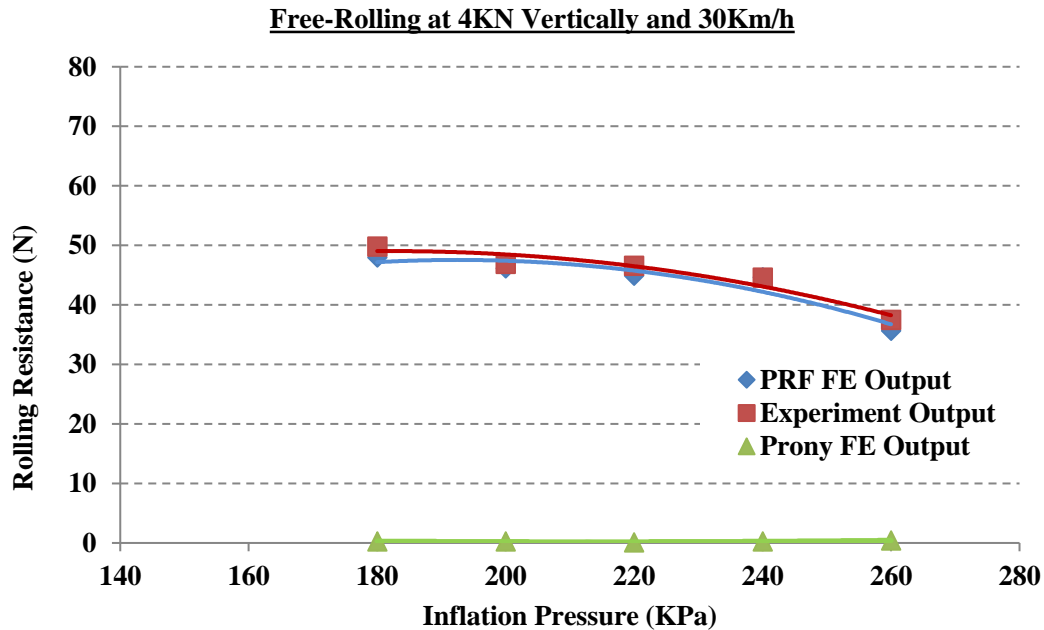


Fig. 7 Impact of inflation pressure over rolling-resistance

which there are negligible changes to the molecules arrangements/entanglement from their equilibrium state. This is agreeing with the views of Dealy and Wissbrun (2012).

Clearly, tire's rolling deformation does not match such a situation since the tire's deformational levels are much larger with a lot higher occurrence rate accompanied with highly non-linear molecules re-arrangements and entanglements inside the tire's rubbery parts. This explains the insensitivity and unresponsiveness of the prony model to the tire rolling conditions in computing the creep dissipation energy of the tire structure.

Regardless, it is possible to implement prony model as an approximation to the tire's viscoelasticity to a limited extent if more prony series coefficients to be used and model's function was successfully fitted to the particular rolling condition under investigation. A task that could be difficult and costly based on the investigated problem complexity and the variety of rolling conditions under investigation (Pelayo *et al.* 2012). As for the PRF model, there is a good match between the PRF and the experimental results for different vertical loading and inflation pressure cases.

The PRF outcomes show that the rolling-resistance is almost linearly proportional to the vertical load. This is as the more the tire is vertically loaded the greater the tire's vertical deflection and its tread curvature distortion would be, during rolling, resulting in larger structure deformation and hence hysteresis losses. This relationship goes in-line with the findings of Hernandez *et al.* (2017) and Rao *et al.* (2006).

On the other hand, with PRF, the rolling-resistance is inversely proportional to the inflation pressure. This is because the greater the inflation pressure of the tire the stiffer it would be, as a result of having more air molecules to fill cavity gaps and support vertical loading, leading to less

vertical deflection and tread's curvature distortion, during rolling, and hence lower structure deformation and hysteresis losses. A similar correlation is found in the works of Hernandez *et al.* (2017) and Rao *et al.* (2006).

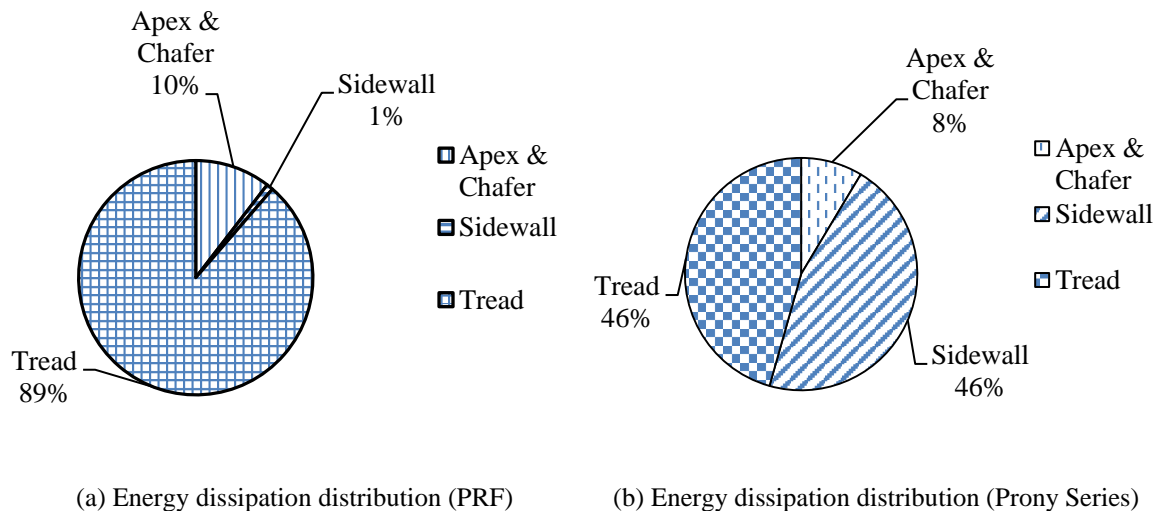


Fig. 8 “ALLCD” distribution over different tire parts

The PRF model shows a reliable energy dissipation distribution among the different tire parts as illustrated in Fig. 8 for example. According to the PRF model and the literature too (Hernandez *et al.* 2017, Akutagawa 2017, Cho *et al.* 2013), the tread is the main tire part that contributes to the rolling-resistance where the sidewall and the apex/chafer contributions are much less. Comparing the sidewall to the apex/chafer, their contribution size could be the same for both or may differ slightly for one of them than the other depending on the tire used. For the investigated tire in this paper, the apex/chafer has a slightly higher contribution to the dissipative energy than the sidewalls.

The close prediction of the PRF to the real tire's rolling-resistance can be attributed to its ability to relate the relaxation rate to the deformational stress and strain responses correctly and account for the non-linearity between the applied stresses and induced strains on a molecular level for a wide deformational range.

7.2 Mechanical comfort (cushioning)

According to Michelin (2002), mechanical comfort due to tire distortion at the contact patch can be assessed through measuring the changes in vertical and lateral forces at the wheel center of a rolling tire on a smooth road drum. Obviously, higher changes would mean more vibrations and greater discomfort and vice versa. After low-pass filtering the data, the assessment results in both PRF and experiment show a close agreement, especially in the vibrational amplitude and frequency. An example on those assessments can be seen in Figs. 9 and 10.

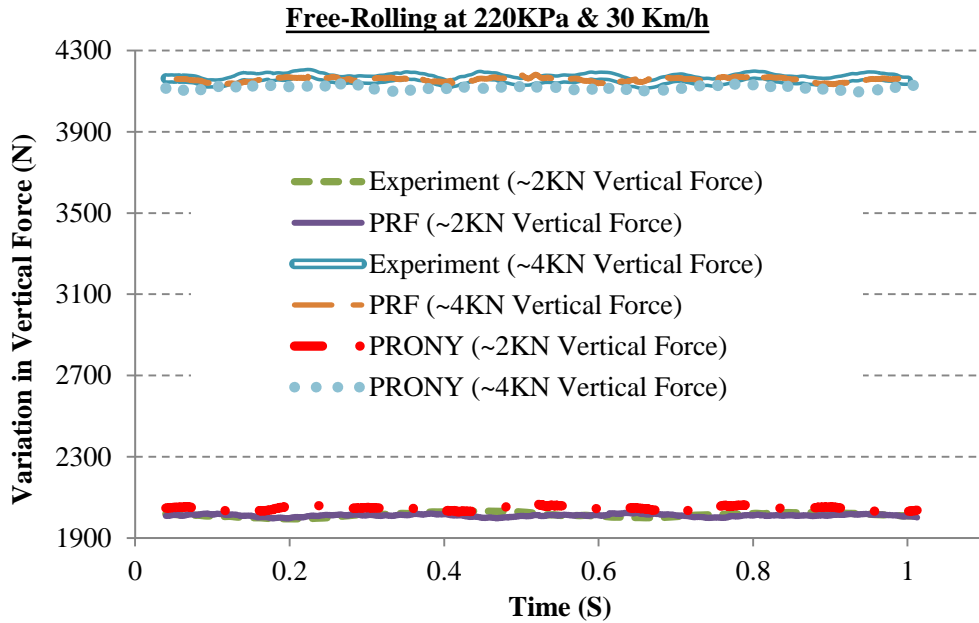


Fig. 9 Variations in vertical force

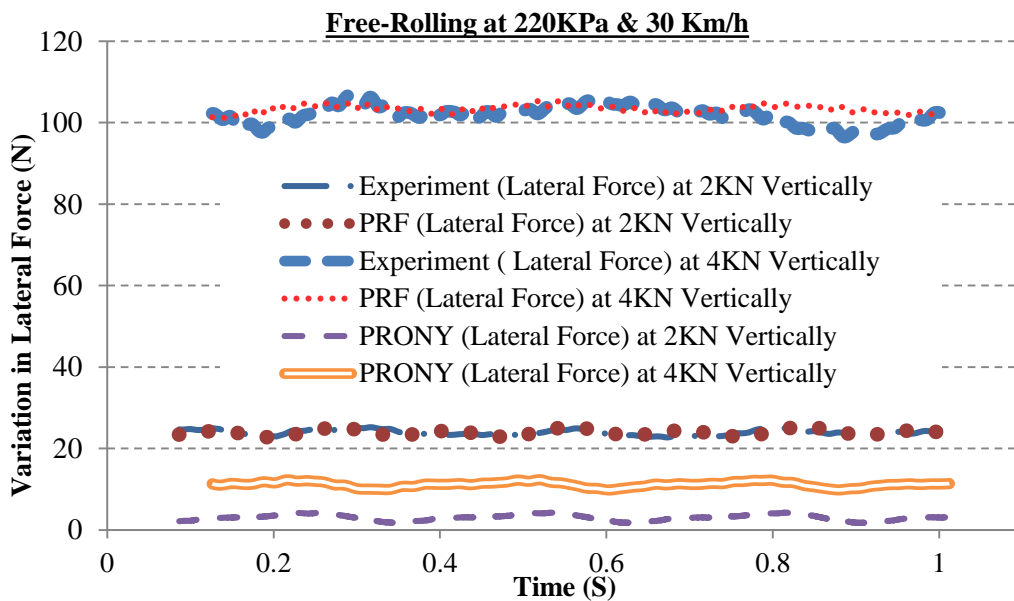


Fig. 10 Variations in lateral force

However, for the prony series results, there is a slight deviation in terms of the vertical vibrational amplitude and frequency compared to the experiments while for the lateral vibrations it illustrates a completely different vibrational amplitude profile.

Such outputs of the prony series may refer due to the model's insensitivity to the intensity of

the axial deformational movements as indicated previously. Vertically at the wheel-center, having a steady-state rolling, the vertical deflection of the tread's contact-patch will be fixed at a certain level with negligible changes due to rolling as it would be sandwiched between the applied vertical load and the fixed/uniform flat road. This condition is within the application scope of the prony series model as there are very small deformational changes vertically at the contact-patch during rolling and shear modulus is considered independent of stress and strain responses. On the other hand, laterally at the contact-patch, the tire's sidewalls will be moving violently due to the peristaltic pumping and their flexibility with almost no movement constraints in place. This situation is clearly outside the applicability scope of the prony model since the deformational changes are large and highly non-linear.

As a result, PRF is found to be capable and more accurate than the prony series in describing the mechanical comfort (cushioning) behavior of the tire during rolling.

8. Conclusions

This paper has investigated the effects of using the PRF model in comparison to the classical prony model on describing the tire's core rolling-resistance and rolling mechanical comfort through a proposed computational approach. In this investigation, the aim was to assess the applicability of the recently introduced PRF model in Abaqus code as a potential and an alternative prediction tool for the tire's internal losses and rolling cushioning which are highly dependent on the tire's material hysteresis.

The results of such investigation verified the validity of the proposed method for rolling-resistance prediction. Another important finding was that the PRF model outperformed the classical prony model in simulating the tire dynamical behavior correctly for both rolling-resistance and rolling cushioning. The PRF results had a close match with that of the relevant experiments while the prony series was unable to predict the right behavior trends except for the vertical mechanical comfort.

Taken together, this paper's findings indicate that the non-linear PRF model is applicable and a better choice than the classical linear prony model for modeling the tire's core rolling-resistance under various vertical loads and inflation pressures respectively. The current findings highlight the potentiality of the PRF model as an alternative prediction tool to better estimate and investigate the rolling-resistance especially due to tire's structural and material effects. Such an approach would enable the tire industry to exclusively evaluate the effects of the tire's geometry, construction and material alone, as design parameters, on the tire's rolling resistance for better tire designing and optimization purposes for low rolling-resistance. This is as the tire's rolling-resistance is growingly driving the tire developments because of its significant impact on vehicle's fuel consumption and CO₂ emissions on a global scale.

However, there is a limitation to the usage of the PRF model, via the explicit procedure, and it is the computational costs incurred depending on the FE model size and the rolling conditions investigated. Nevertheless, in addressing and minimizing such a limitation, the authors advise to use the proposed method of rolling-resistance prediction, have the proper computational resources, or use "mass-scaling" technique if necessary.

The slight differences between the PRF and the experimental results can be attributed to the disregard of the effects of the tread pattern and the reinforcement's viscoelasticity in the FE simulation, the FE solution noises and the real tire's shape/structure non-uniformity due to

manufacturing imperfections. As a future work, the authors look forward to using the developed PRF FE model as a platform for tire prototype designing for low rolling-resistance.

References

- Akutagawa, K. (2017), "Technology for reducing tire rolling resistance", *Tribology Onl.*, **12**(3), 99-102.
- Aldhufairi, H.S. and Olatunbosun, O.A. (2017), "Developments in tyre design for lower rolling resistance: A state of the art review", *J. Automob. Eng.*, **232**(14), 1865-1882.
- Andersen, L.G. (2015), "Rolling resistance modelling: From functional data analysis to asset management system", Ph.D. Dissertation, Roskilde Universitet, Denmark.
- Andersen, L.G., Larsen, J.K., Fraser, E.S., Schmidt, B. and Dyre, J.C. (2014), "Rolling resistance measurement and model development", *J. Transp. Eng.*, **141**(2), 04014075.
- ASTM (2014), *E328-13, Standard Test Methods for Stress Relaxation for Materials and Structures*, ASTM International, West Conshohocken, Pennsylvania, U.S.A.
- ASTM (2016), *D412-15a, Standard Test Methods for Vulcanized Rubber and Thermoplastic Elastomers-Tension*, ASTM International, West Conshohocken, Pennsylvania, U.S.A.
- Cho, J., Lee, H., Jeong, W., Jeong, K. and Kim, K. (2013), "Numerical estimation of rolling resistance and temperature distribution of 3-D periodic patterned tire", *Int. J. Sol. Struct.*, **50**(1), 86-96.
- Clermont-Ferrand, M. (2003), *The Tyre: Rolling Resistance and Fuel Savings*, Société de Technologie.
- Dealy, J.M. and Wissbrun, K.F. (2012), *Melt Rheology and Its Role in Plastics Processing: Theory and Applications*, Springer Science & Business Media.
- Ghosh, P., Saha, A. and Mukhopadhyay, R. (2003), "Prediction of tyre rolling resistance using FEA", *Constit. Mod. Rubb.*, 141-146.
- Ghosh, S. (2011), "Investigation on role of fillers on viscoelastic properties of tire tread compounds", Ph.D. Dissertation, Maharaja Sayajirao University of Baroda, India.
- Heeps, G. (2015), *Another Fine Mesh*, Tire Technology International, 50-56.
- Hernandez, J.A., Al-Qadi, I.L. and Ozer, H. (2017), "Baseline rolling resistance for tires' on-road fuel efficiency using finite element modeling", *Int. J. Pave. Eng.*, **18**(5), 424-432.
- Hoever, C. (2014), "The simulation of car and truck tyre vibrations, rolling resistance and rolling noise", Ph.D. Dissertation, Chalmers University of Technology, Sweden.
- ISO (2005), *ISO 18164:2005, Passenger Car, Truck, Bus and Motorcycle Tyres-Methods of Measuring Rolling Resistance*, International Standard, Switzerland.
- Jae, E. (2015), "Data directory: Future market insights on specialty silicas", *Tire Technol. Int.*, **70**.
- Katz, J. (2016), *Automotive Aerodynamics*, John Wiley & Sons, West Sussex, U.K.
- Li, Z., Li, Z.R. and Xia, Y.M. (2012), "An implicit to explicit FEA solving of tire F&M with detailed tread blocks", *Tire Sci. Technol.*, **40**(2), 83-107.
- Michelin (2002), *The Tyre: Mechanical and Acoustic Comfort*, Société de technologie Michelin.
- Nandi, B., Dalrymple, T., Yao, J. and Lapczyk, I. (2014), "Importance of capturing non-linear viscoelastic material behavior in tire rolling simulations", *Presented at the Meeting of the Tire Society*, U.S.A., September.
- Narasimha Rao, K., Kumar, R.K. and Bohara, P. (2006), "A sensitivity analysis of design attributes and operating conditions on tyre operating temperatures and rolling resistance using finite element analysis", *J. Automob. Eng.*, **220**(5), 501-517.
- Pelayo, F., Noriega, A., Lamela, M.J. and Fernández-Canteli, A. (2012), *Comparison of Viscoelastic Moduli Fitting Using Optimization Methods*, ECF19.
- Redrouthu, B.M. and Das, S. (2014), "Tyre modelling for rolling resistance", M.Sc. Dissertation, Chalmers University of Technology, Sweden.
- Schuring, D. (1977), "A new look at the definition of tire rolling loss", *Tire Rolling Losses and Fuel Economy-An R&D Planning Workshop*, Warrendale, Pennsylvania, U.S.A.

- Smith, G. and Blundell, M. (2017), “A new efficient free-rolling tyre-testing procedure for the parameterisation of vehicle dynamics tyre models”, *J. Automob. Eng.*, **231**(10), 1435-1448.
- Steen, V.D.R. (2010), “Enhanced friction modeling for steady-state rolling tires”, Ph.D. Dissertation, Technische Universiteit Eindhoven, the Netherlands.
- Systèmes, D. (2013a), *Abaqus Analysis User's Guide, 22.5.1 Hyperelastic Behavior of Rubberlike Materials*, Providence, Dassault Systèmes Simulia Corp., Rhode Island, U.S.A.
- Systèmes, D. (2013b), *Abaqus Analysis User's Guide, 22.7.1 Time Domain Viscoelasticity*, Providence, Dassault Systèmes Simulia Corp., Rhode Island, U.S.A.
- Systèmes, D. (2013c), *Abaqus Analysis User's Guide, 22.8.2 Parallel Rheological Framework*, Providence, Dassault Systèmes Simulia Corp., Rhode Island, U.S.A.
- Systèmes, D. (2013d), *Abaqus Analysis User's Guide, 6.3.3 Explicit Dynamic Analysis*, Providence, Dassault Systèmes Simulia Corp., Rhode Island, U.S.A.
- Wei, C. (2015), “A finite element based approach to characterising flexible ring tire (FTire) model for extended range of operating conditions”, Ph.D. Dissertation, University of Birmingham, U.K.
- Yang, X. (2011), “Finite element analysis and experimental investigation of tyre characteristics for developing strain-based intelligent tyre system”, Ph.D. Dissertation, University of Birmingham, U.K.